183

Egypt. J. Chem. **Vol. 66,** No. 5 pp. 25 - 34 (2023)

Egyptian Journal of Chemistry

Synthesis, characterization of chitosan based green Hyperbranched Polymers/Reduced Graphene Oxide Composites

Amira.M.Qassem[1*], Khalid I.Kabel [1] , Ahmed A. Farag 1, Mohamed Keshawy [1,] Abdulraheim M.A.Hassan[1] and Eman H. Ismail[2]

[1]Petroleum Applications Department, Egyptian Petroleum Research Institute, Cairo, Egypt.
[2] faculty of science ,chemistry department ,Ainshams university ,Cairo,Egypt.

Abstract

A new series of sorbent materials comprised of green hyper-branched polymer and reduced graphene oxide was prepared. The hyperbranched polymer was synthesized by a three-step reaction of chitosan (extracted from shrimp shells) with 2-chloroethyl amine hydrochloride to give three generations denoted as G1, G2, and G3 (the hyperbranched polymer). G3 was used to form different composites with reduced graphene oxide (rGO). rGO was synthesized from graphite powder by modified Hummer's Method followed by the reduction of GO with hydrazine hydrate. The composites were denoted as HBP/rGO$_{0-2}$ for rGO from 0 to 2 wt % respectively. The grafting reaction was confirmed by FTIR. The morphology of the composites was monitored via scanning electron microscopy (SEM). Other properties such as the thermal properties and the crystallinity of the prepared composites were also investigated by the thermal gravimetric analysis (TGA) and X-ray diffraction (XRD) analysis respectively. The prepared hyperbranched polymer can be used in important applications as will be seen in next researches.

keywords: Chitosan, chloro ethyl amine, reduced graphene oxide, green composite, characterization.

1. Introduction

polysaccharides are regarded as one of the most significant classes of biomaterials Due to their biocompatibility, adaptability, and similarity to natural extracellular matrix (ECM), In tissue engineering applications, several polysaccharides are employed and studied. One of the most naturally produced polysaccharides with numerous intriguing uses is chitosan. Due to its low price, high adsorption capacity in comparison to other sorbents[1], it is regarded as an efficient bio-sorbent. Some fungai species' cell walls include it; nevertheless, commercial chitosan can be produced in large quantities and at low cost from chitin, which ranks second only to cellulose in terms of abundance in nature.[2-4] Chitosan is a fascinating biomaterial with exceptional qualities, such as biocompatibility, biodegradability, antibacterial activity, and low immunogenicity, as well as adaptability, hygroscopicity, and similarity to moisturising properties and native extracellular matrix

(ECM). These characteristics have led to its widespread use in pharmaceuticals, food preservation, environmental cleanup [5], and other industries. As the application fields continue expanding, versatile, chitosan derivatives and their corresponding modification technologies have been developed to satisfy the very need of modern society[4, 6].Hyper branched polymers (HBPs) are one of the most significant chitosan modification technologies, which are major research topics with a great deal of interest from both industrial and academic researches Their high degree of branching, lower viscosity, greater solubility due to high functionality, high capabilities for absorbing pollutants, and ability to be grafted by a variety of chemicals make them superior to other sorbent materials Due to the abundance of amino functional groups that terminate the branching in HBPs (including hydroxyl amine, amino, and amide groups) [7-11], these compounds are active in a variety of reactions and applications. Chitosan was proposed in

this study to construct the hyperbranched polymer. Chitosan is chosen because of its superior. Based on its greater advantages, as outlined above, it can be modified to create thin films, fibres, gels, sponges, beads, or polymeric materials based on nanoparticles . In our work**:** halo alkyl amine and reduced graphene oxide were used to modify chitosan as reduced graphene oxide has been a topic of both intense and broad investigation Due to its exceptional mechanical, electrical, optical, and thermal capabilities[12, 13]. The increase in electric conductivity up to 6300 S cm $^{-1}$ and high mobility of 320 cm^2 V1 s 1 are two of the most significant results of the GO reduction process. During the reduction phase, rGO's surface area likewise grows. With a Young's modulus of 1.0 TPa and a breaking strength of 130 GPa, which is comparable to graphene, rGO sheets exhibit remarkable mechanical strength[7, 14]. Due to the higher C/O ratio of the structure than GO, reduced graphene oxide develops a hydrophobic characteristic. The hydrophobicity of rGO causes a decrease in this material's dispersibility after reduction[12, 15]. Additionally to The reduction process lowers the critical coagulation concentration, which has an impact on the colloidal behaviour of rGO in addition to its dispersibility. Even though the reduction of GO does not completely restore the graphene structure[16-18], The desirable characteristics of graphene oxide continue to exist, including tunable functionality, high electric and thermal conductivity, the availability of starting material, and an affordable and scalable manufacturing method Reduced graphene has also been using as reinforcement material to improve various properties of many polymers. Such as Polyvinyl alcohol (PVA) and HBPs which offers many properties to be improved. Our work aimed to well grafting of reduced graphene in HBP matrix (chitosan derivative or chitosan halo alkyl amine). On which efficiency of reinforcement depends, surface morphology and crystallinity was **improved.**

Experimental
2.1. Materials

Shrimp shells were obtained as waste materials. Other materials used throughout this work are listed in Table 1.

Table 1: Different materials used in this work

Material	Description and Source	Material	Description and Source
Acids and bases			
Sodium hydroxide	Analytical grade reagents obtained from Biochem.	Hydrochloric acid	Analytical grade reagents obtained from Biochem.
Ammonia solution (0.25wt%)		Sulphuric acid	
Chloroethyl amine hydrochloride (CEA)		Acetic acid	
Other materials			
Graphite	Local source	Acetone	Analar, Biochem.
Hydrazine hydrate	Analar, Biochem	H_2O_2	Biochem

2.2. Methodology:

2.2.1. Obtaining chitosan from shrimp shells:

The following experimental procedures were carried out to extract chitin from shrimp shells then converting into chitosan:

The raw shrimp shells were cleaned with running water and then drenched in a plenty amount of distilled water for 1.5 hours at 60ºC with continuous stirring. The shells were then dried in an oven (Schimatzu Copr.) at 60°C till complete dry. The shells are experienced the following processing:

- **Deproteination:**

The deproteination was conducted by treating the dried shrimp shells with 3% (w/v) sodium hydroxide at a ratio of 1:18(w/w) for 3 hours at 80°C. The proteins were removed by decantation. The treated shells were dried in a drying oven at 60°C for 10 hours.

- **Demineralization:**

It was carried out by treating the deproteinated shells with 3M hydrochloric acid at a ratio of 1:18 (w/w) for 3hours at 25°C. Chitin was obtained by decantation and was dried in the oven at 60°C for 10hours.

- **Deacetylation of chitin into chitosan:**

Deacetylation was carried out by treating chitin with 50% (w/w) sodium hydroxide at a ratio of 1:18 (w/w) for 3hours at 80°C. The product chitosan was obtained by filtration[19].The chitosan was washed several times to remove alkali. The average molecular weight of the extracted chitosan as estimated by the GPC was 166666.667 g/mole with degree of deacetylation 78%.

2.2.2. **Preparation of chitosan hyperbranched polymer** (reaction of chitosan with chloroethyl amine) The hyperbranched polymer with the third degree of branching was obtained by a step-growth approach between chitosan and chloroethyl amine as following[20]

a- Preparation of G_1
3.2 gm (0.028 mole) of chloroethylamine **hydrochloride** was dissolved in 50ml DH_2O in a 100 m flask which was charged with 2gm (0.012M) of **chitosan which is dissolved in 2% acetic acid** and the mixture was stirred at 65^0C for **8 h** hours then the product was cooled at room temperature. After that, 7ml of 30% NaOH was added with refluxing at 95^0C. The resultant was washed with acetone then the solvent was evaporated and the product was dried at an oven for 6 h at 65^0C.

b- Preparation of G_2
6.38 gm (0.0558 mole) of 2-chloroethyl amine **hydrochloride** and 2.4 gm (0.06 mole) of NaOH were dissolved in 25ml DH_2O and the solution was kept at 10^0C for 30 min. Then, 1gm of G_1 was added with continuous stirring for **3h** hr. at 55^0C. Afterwards, additional 7ml of 30% NaOH was added to the previous flask and the reaction is hold at 90^0C for 5 hr. After completion, the reaction was allowed to cool to room temperature. G_2 was separated by filter paper and dried in vacuum oven for 48hr a temp 60^0C.

c- Preparation of G_3
The same procedure was followed between 2-**chloroethyl amine hydrochloride** and G2 with the same amounts. The polymer was obtained by filtration and the product was dried in vacuum oven for 48hr at a temp 60^0C.

2.2.3. Preparation of GO (graphene oxide)
Graphite was crushed to tiny particles of average size 20-25 µm by mechanical cleavage (ball mill). Graphene oxide was synthesized from the natural Graphite powders following a modified Hummer's and Offenman's method[21]. Briefly, 0.5g graphite powder was pre-oxidized with a mixture comprised of 23 ml of concentrated H_2SO_4 and 0.5 g $NaNO_3$. The mixture was then stirred in an ice bath for about 4 h. Then, 3 g of $KMnO_4$ was added slowly into the mixture with an interval of 15 minutes with vigorous stirring for 1 hour. The solution was heated slowly to above 35°C and 45 ml of distilled water is added into the solution which was cooled to room temperature and continued stirring for 1 h. The temperature of the mixture was raised to 90°C and kept constant for 2 h with stirring. Afterwards, 100 ml distilled water was added into the solution. The reaction was stopped by the addition of 10 – 15 ml of 30% H_2O_2. The mixture was washed with 100 ml of 5% HCl solution and allowed to settle down for about 24 hours. In order to remove all the impurities, the mixture was washed with distilled water several times and repeatedly centrifuged at 5000 rpm for 10 minutes. After centrifuging, the filtrate was dried at 60 °C to obtain black powder.

2.2.4. Reduction of GO by hydrazine hydrate into rGO.
The graphene oxide was reduced by the addition of 1-3 drop of hydrazine hydrate into a solution of 3gm GO in 10ml DH_2O. Then, the solution was boiled with continuous stirring for 30 minutes. The reduced graphene oxide (rGO) was obtained by filtration [22].

2.2.5. Grafting of rGO on hyper branched polymer
Chitosan HBP/rGO composites were obtained by grafting different weight ratios of rGO into the hyperbranched polymer according to the following experimental steps:
1gm of G_3 was dissolved in (50 ml of 2% acetic acid) to which the desired amount of rGO (0.5, 1, 1.5 and 2 weight percent) was added and the mixture was sonicated for 2 at ambient temperature. Afterwards, 50 ml of 0.25 wt% of ammonia solution was dropped into the solution with continuous stirring. The solution is filtered and the filtrate was washed with DH_2O and dried at **50 °C** for 10 hrs.
The codes and the composition of the prepared composites are given in Table 2.

Table 2: Codes and composition of chitosan based HBP/rGO composites.

Code	G3 (gm)	rGO (wt.%)
HBP/rGO$_{0.5}$	1	0.5
HBP/rGO$_1$	1	1
HBP/rGO$_{1.5}$	1	1.5
HBP/rGO$_2$	1	2

2.3. Characterization.
2.3.1. FTIR spectroscopy
The Fourier Transform Infrared (FTIR) Analysis were carried out by using FTIR, Model (thermo scientific Nicolet iS10 spectrometer) produced by thermo fisher scientific (USA) Company in spectral range from 4000 cm-1 to 400 cm^{-1}, beam splitter is KBr/Ge mid infrared optimized, with resolution 4 cm^1.

2.3.2. ^{1}HNMR spectroscopy:

The chemical modification reactions and the preparation protocols were further confirmed by ^{1}HNMR spectroscopy. The spectra were recorded on NMR Model Bruker high performance digital FT-

_____

NMR spectrometer Avance III 400MHZ. Performing routing 1H/13C high –resolution spectra along with common 2D experiments (Cosy, HMBC, HSQC) and x-nucleus experiments.

2.3.3. Scanning electron microscopy (SEM)
The surface morphology of the dried composites was studied by using scanning electron microscope model (Zeiss evo 10) attached with EDX Unit (Energy Dispersive X-ray Analyses), with accelerating voltage 500 K.V., magnification14x up to 100000x.

2.3.4. Atomic force microscopy investigation:
The surface morphology, topography and roughness were investigated by using Nanosurf, Flexaxiom AFM. The scanning process was conducted at room temperature by phase contrast mode by using NCLR cantilever.

2.3.5. Thermal gravimetric analyses (TGA)
TGA were conducted on Perkin-Elmer TGA7 thermo balance. The dried samples were analyzed under nitrogen atmosphere in the temperature range of 50–600ºC at scanning rate of 20 ºC /min.

2.3.6. X-ray diffraction analysis:
X-ray diffraction patterns of the prepared composites were performed by using an X-ray diffractor unit (Philips PW3040/60 X'pert PRO PANalytical-Netherlands). The samples were placed on a glass slide and the measurements were taken continuously from 5to 90 angles.

3.   Results and discussion:

3.1.   Preparation of chitosan- based hyperbranched/rGO composites:
The extraction of chitin from crustaceans' shells and deacetylation into chitosan was the topic of many studies. The quality and physical properties of chitosan are dependent on the conditions of the chemical extraction process

Hossain and Iqbal obtained chitosan with high molecular weight (1.05×10^6 Dalton), and high degree of deacetylation (81.24%) by drastic alkaline (60% NaOH for 24 hours at 60°C) treatment of chitin isolated from shrimp shells[23]. This type of chitosan is not suitable for constructing hyperbranched polymer due to the steric hindrance of the crowded amino groups on which the branches are built Therefore, we applied mild conditions to convert the chitin extracted from shrimp shells into chitosan. The overall protocols of extraction and conversion are represented in Figure 1a.

The second preparation step involves building up the chitosan-based hyperbranched polymer via three subsequent grafting reactions with chloroethyl amine, Figure 1b. Chitosan modified hyperbranched polymers were synthesized for different applications[24, 25]. Chen et al[24, 26] prepared hyper branched polymers by grafting poly acrylic acid-co-acrylamide onto chitosan backbone to obtain polymers of high degree of branching for enhanced oil recovery. Guzman et al [25] introduced imine-chitosan derivatives for heavy metal removal. In the present work, the hyperbranched polymer was prepared by successive simple grafting of reaction chloroethyl amine accompanied by elimination of HCl. This modification produced high water -soluble chitosan derivative to fit the desired application. In order to obtain maximum removal efficiency versus different species, reduced graphene oxide was incorporated into the claimed HBP. Reduced graphene oxide was proved as an effective sorbent material towards different pollutants due to its high surface area, and high functionality[27, 28]. It is prepared by oxidation of graphite into graphene oxide then reduction by hydrazine hydrate, Figure 1c. The final step of preparation of hyperbranched polymer/reduced graphene oxide is presented in Figure 1d.
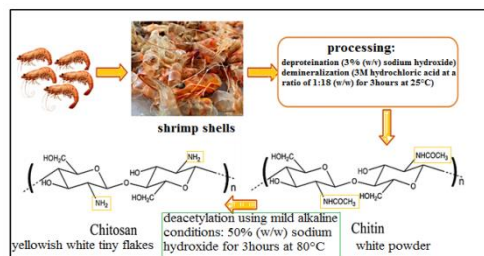

Figure 1a: Extraction of chitin from shrimp shells and deacetylation of chitin into chitosan
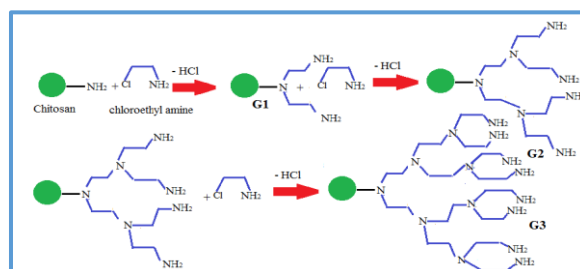

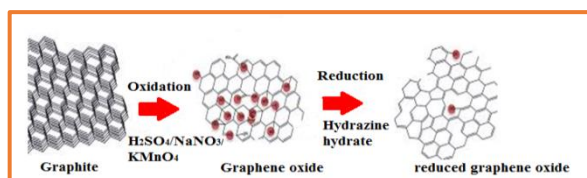**Figure 1b: Synthesis of chitosan-based hyperbranched polymer**

_____
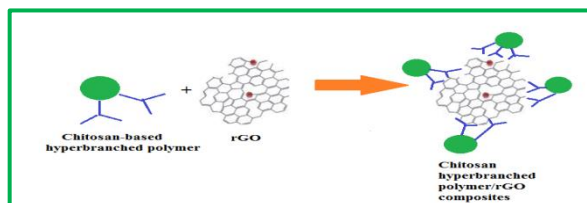
Figure 1c: Preparation of rGO from graphite.

Figure 1d: Preparation of green chitosan-based/rGO composite

3.1.1. FT-IR Characterization

The FTIR spectra of chitosan, G1, and G3 are illustrated in Figure 2. The IR spectrum of chitosan depicts the following absorption peaks: A wide peak at between 3300-3500 cm^{-1} due to the stretching vibrations of overlapped NH$_2$ and O-H groups. Another peak is shown **at 2878 cm^{-1} assigned to C-H stretching. the peak at**

1580 cm$_{-1}$ could be assigned to N–H bending vibration , The significant peak of the carbonyl group of (CONH$_2$) is slightly shifted to 1650 cm^{-1} due to the intramolecular hydrogen bonding within the chitosan molecule. On the other hand, the spectra of G$_1$ and G3 show the same absorption bands with slight shifts due to chain extension. For instance, the peak assigned for carbonyl group is shifted from 1650

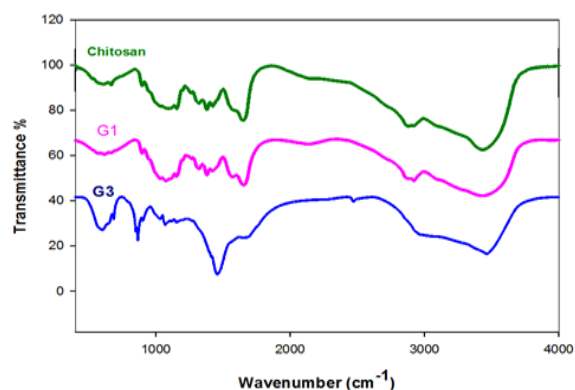cm^{-1} in the spectrum of G1 to 1660 cm^{-1} in the spectrum of G3.

Figure 2: The FTIR spectra of chitosan, G1 and G3.

3.1.2. ^{1}HNMR characterization:

Magnetic resonance analysis is one of the most important methods to confirm the chemical structure. In this regard, the ^{1}HNMR of chitosan, G1, G3 and G3-rGO$_{0.5}$ are illustrated in Figure 3a-d respectively. Moreover, the ^{1}HNMR outcomes are tabulated in table 3. The given spectra provide a comprehensive outlook to confirm the chemical modification of chitosan. For instance, the spectrum of chitosan depicts 3 peaks for three types of non-equivalent protons and the integration of each peak is assigned for the number of protons for that peak. In the spectrum of G1, the peaks

Table 3 ^{1}HNMR data of some investigated samples (S= singlet, d= doublet, t= triplet, q=quartet, m=multiplet)

Compound	Chemical shift (δ, ppm)	Peak Integration	Interpretation
Chitosan	1.6, t	2	Protons of amine group
	2.4, d	4	Protons of hydroxyl group
	3.6, s	4	Protons of hexose ring
G1	0.5, t	4	Protons of CH$_2$ adjacent to 3ry nitrogen
	0.9, t	4	Protons of CH$_2$ adjacent to NH$_2$ group
	1.6, t	4	Protons of NH$_2$ group
	2.6, d	4	Protons of OH group
	3.5, s	4	Protons of hexose ring
G3	1.4, m	12	Protons of the CH$_2$ of the branched chain adjacent to 3ry nitrogen
	2.5, m	12	Protons of the CH$_2$ of the branched chain adjacent to NH$_2$ group
	3, triplet overlapped with neighboring peak	12	Protons of the NH$_2$ group
	3.3, overlapped	4	Protons of the OH group
	3.7, overlapped	4	Protons of the hexose ring
G3-rGO0.5	0.7-1.4, m	12	Protons of the CH$_2$ of the branched chain adjacent to 3ry nitrogen
	1.6-1.8, m	12	Protons of the CH$_2$ of the branched chain adjacent to NH$_2$ group
	2.2-2.4, m	12	Protons of the NH$_2$ groups
	3.1-3.5, overlapped with neighboring peak	4	Protons of the OH groups of the hexose ring
	3.6-3.9, overlapped with neighboring peak	4	Protons of the hexose ring
	5.2-5.5, m	14	Protons of the OH groups of reduced graphene oxide

assigned for two non-equivalent methylene groups appear in the region of 0.5-0.9 δ with the integration of 12 protons for each group which confirms the successful formation of the first branched structure. On the other hand, peak shifting and overlapping are noticed in the spectrum of G3 due to the emergence of the hyperbranched structure. The composite formation between G3 and rGo is confirmed by the occurrence of the protons of OH groups of the GO in the spectrum of G3-rGO0.5.
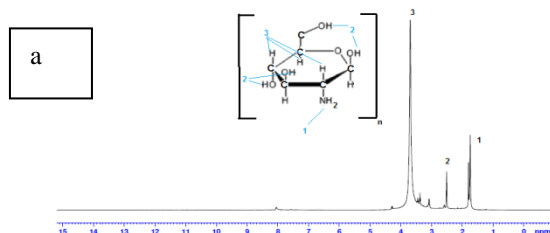
Figure 3a -¹HNMR of Chitosan
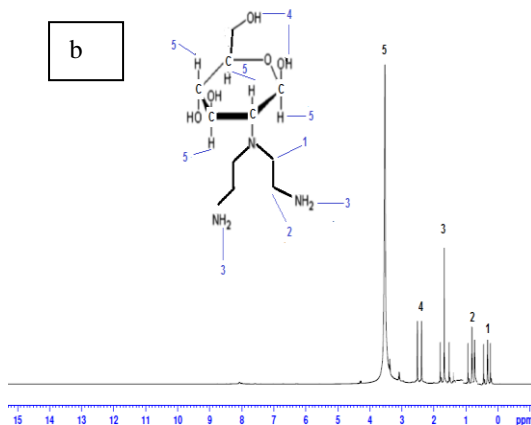
Figure 3b -¹HNMR of G₁

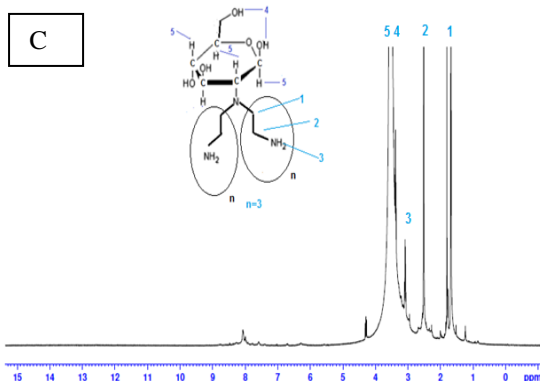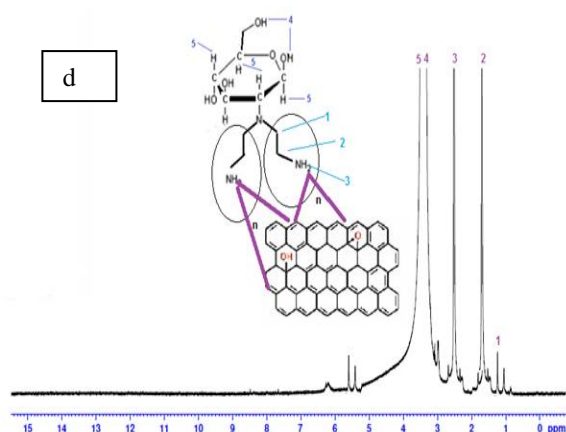**Figure 3c -¹HNMR of G₃**

Figure 3: ¹HNMR of a) chitosan, b) G1, c) G3 and d) G3-rGO₀.₅

3.1.3. Surface morphology via Scanning electron microscope

The surface morphology of the chitosan, G_3 and HBP/rGO$_{0.5}$ was investigated via the SEM, Figure 4 a-c. The SEM micrograph of chitosan displayed the semicrystalline nature of chitosan, Figure 4a. On the other hand, the surface morphology of G3 exhibited porous appearance with uniform pores. The image of HBP/rGO$_{0.5}$ demonstrated numerous pores with graphene oxide particles scattered within the matrix. This observation may be explained by the change in the crystalline nature of chitosan by chemical adaptation into hyperbranched polymer.
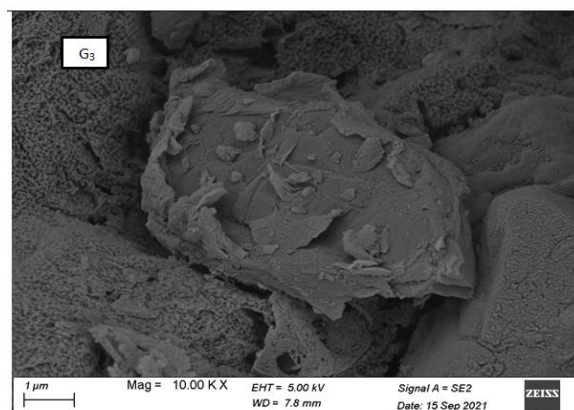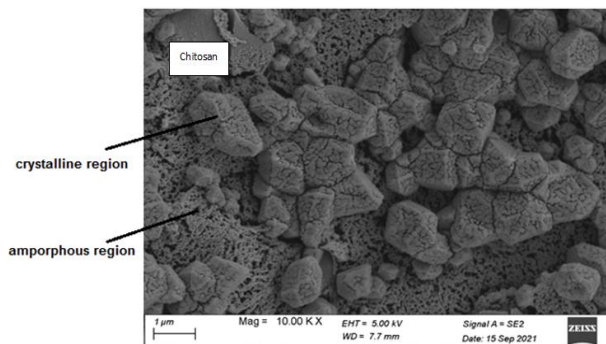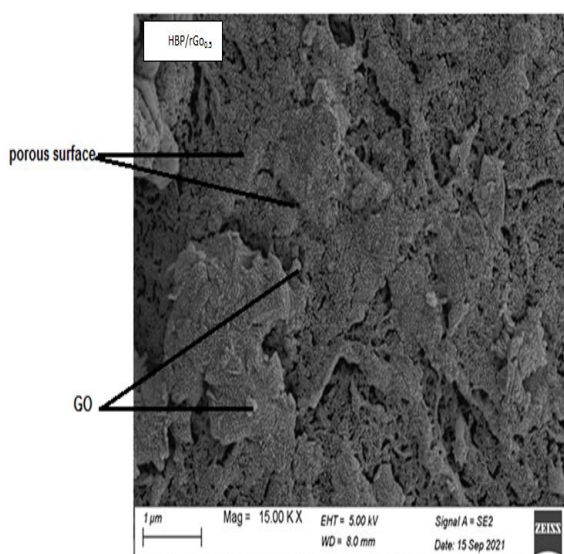
Figure 4: SEM micrographs of chitosan, G3 and HBP/rGO$_{0.5}$.

3.1.4. AFM topographic investigation:

The surface modification of chitosan can be monitored via the AFM by comparing the changes that occurred on the surface topography[29]. In this regard, the AFM images of chitosan, G3 and HBP/rGO$_{0.5}$ are illustrated in Figure 5 a-c respectively. There are three main AFM outputs used to achieve the investigation, namely, the topography of the surface, the height represented by the Z-axis to measure the difference between the maximum point above the surface and the minimum point below the surface and the roughness measurements to display Physico-chemical changes that befallen to the inspected samples. Some data outcomes are tabulated in Table 4. It can be seen that both the height and the roughness of chitosan increase by the chemical modification into the hyperbranched structure. Also the parameters of the composite [30]including the graphene oxide are much greater than those for the hyperbranched counterpart.

Table 4: Some AFM data for the investigated samples

Compound	Height (nm)	Roughness (nm)
Chitosan	2.09	22.7
HBP (G3)	103	39.8
HBP/rGO$_{0.5}$	124	52.2
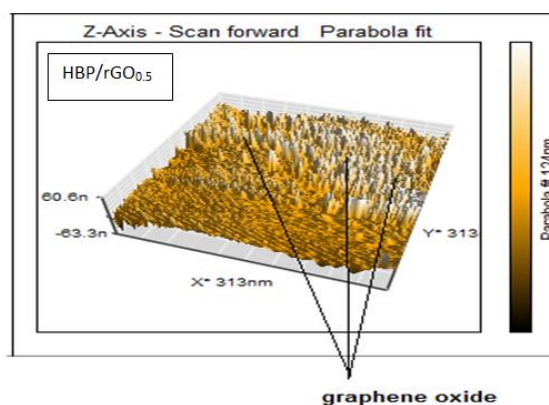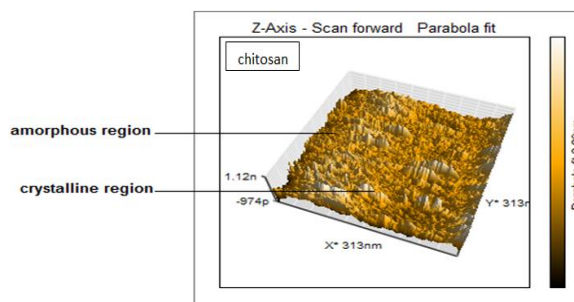
Figure 5: AFM images of chitosan, G3 and HBP/rGO$_{0.5}$.

3.1.5. X-ray diffraction.

The crystallinity of chitosan, HBP, HBP/rGO$_{0.5}$, and HBP/rGO$_{1.5}$ was investigated via the XRD, Figure 6. The diffraction pattern of chitosan depicts two significant angles of crystallization, one appears at positions 12.0° and the other 20.0°. They reflect the semi-crystalline nature of chitosan due to the intramolecular hydrogen bondings. On the other hand, the XRD pattern of HBP showed an amorphous structure due to the destruction of the intramolecular hydrogen bondings of chitosan as a result of the formation of a hyperbranched structure. However, the XRD of HBP/rGO$_{(0.5\ w\%)}$ reveals more crystallinity than HBP [31, 32] due to the crystallographic shape of rGO platelets which allow the molecules of HBP to arrange regularly between its sheets. Hence the

rigidity and crystallinity of HBP increase, by increasing of rGO to 1.5w% percent; the crystallinity increases resulted in more diffraction angles
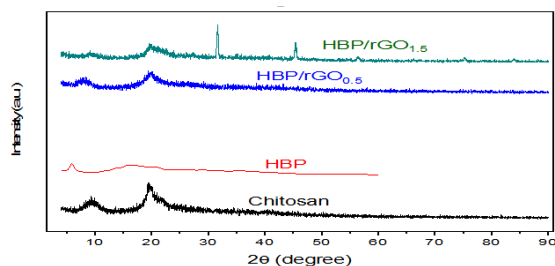

Figure 6: The XRD pattern of chitosan, HBP, HBP/rGO$_{0.5}$, and HBP/rGO$_{1.5}$.

3.1.6. Thermal gravimetric analysis (TGA)

The degradation patterns of chitosan -Figure 7- displayed two stages of thermal decomposition, the first stage lies between 0°C to 170 °C with weight loss 13% due to the loss of adsorbed and bound water, the second stage ranged from 210°C to 400°C with weight loss 78% due to the decomposition of chitosan polymer chains[33-35].

On the other hand, the thermogram of G3 showed two degradation stages, one in the range from 120°C to 250 °C with weight loss about 20 % corresponds to the loss of adsorbed and bound water, the second stage ranged from 300 °C to 410°C with weight loss 60% due to the decomposition of polymer chain. The difference in degradation stages proved that the chitosan modified hyperbranched polymer exhibited higher stability than the chitosan itself However, the thermal degradation patterns of two hyperbranched (HBP/rGO$_{0.5}$ and HBP/rGO$_{1.5}$) composites were investigated. The graphs for both composites showed higher thermal stability due to the incorporation of different percentages of rGO. The two degradation stages for both composites are shifted towards higher temperatures. The degradation stages, weight loss for each stage and T50 for the investigated samples are recorded in Table 5. It is obvious that T50 of HBP/rGO$_{1.5}$ is 380°C.

Table 5: TGA data of selected samples

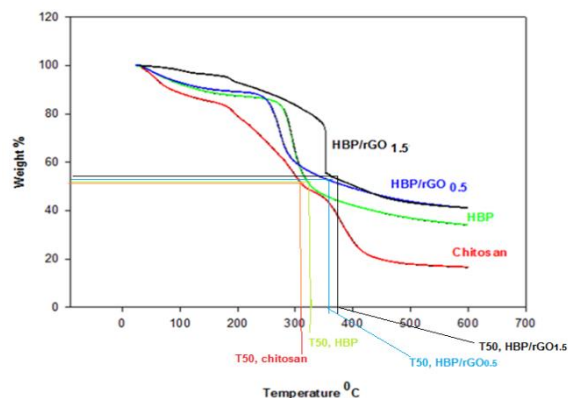| Sample	1st degradation (°C)	Weight loss (%)	2nd degradation (°C)	Weight loss (%)	T50 (°C)
Chitosan	0-170	13	210-400	78	305
G3	120-250	20	300-410	60	325
HBP/rGO$_{0.5}$	160-300	10	310-600	55	355
HBP/rGO$_{1.5}$	200-370	20	370-600	45	380

Figure 7: TGA thermograms for chitosan, G3, HBP/rGO$_{0.5}$, HBP/rGO$_{1.5}$.

4. Conclusion

The study explained the preparation of (green composite HBP/rGO) hyper branched polymer grafted reduced graphene oxide. Chitosan, HBP and HBP/rGO was analyzed by XRD, FTIR, TGA, and SEM, NMR and AFM which determines good reaction between chitosan and chloro ethyl amine hydrochloride to produce HBP, and also determine well grafting of rGO along HBP chain to produce the composite (HBP/rGO).the prepared composite can be used as a good candidate for removing of heavy metals from petroleum waste water.

References:

1. Li, S., et al., *Molecular modification of polysaccharides and resulting bioactivities.* Comprehensive Reviews in Food Science and Food Safety, 2016. 15(2): p. 237-250.
2. Darge, H.F., et al., *Polysaccharide and polypeptide based injectable thermo-sensitive hydrogels for local biomedical applications.* International journal of biological macromolecules, 2019. 133: p. 545-563.
3. Yang, L. and L.-M. Zhang, *Chemical structural and chain conformational characterization of some bioactive polysaccharides isolated from natural sources.* Carbohydrate polymers, 2009. 76(3): p. 349-361.

4. Rinaudo, M., *Chitin and chitosan: Properties and applications.* Progress in polymer science, 2006. 31(7): p. 603-632.

5. Pakdel, P.M. and S.J. Peighambardoust, *Review on recent progress in chitosan-based hydrogels for wastewater treatment application.* Carbohydrate polymers, 2018. 201: p. 264-279.

6. Wang, J. and S. Zhuang, *Chitosan-based materials: Preparation, modification and application.* Journal of Cleaner Production, 2022: p. 131825.

7. Kosowska, K., et al., *Chitosan and graphene oxide/reduced graphene oxide hybrid nanocomposites–Evaluation of physicochemical properties.* Materials Chemistry and Physics, 2018. 216: p. 28-36.

8. Liu, W., et al., *C-coordinated O-carboxymethyl chitosan metal complexes: Synthesis, characterization and antifungal efficacy.* International journal of biological macromolecules, 2018. 106: p. 68-77.

9. Tu, H., et al., *Highly cost-effective and high-strength hydrogels as dye adsorbents from natural polymers: chitosan and cellulose.* Polymer Chemistry, 2017. 8(19): p. 2913-2921.

10. Wang, W., et al., *Chitosan derivatives and their application in biomedicine.* International journal of molecular sciences, 2020. 21(2): p. 487.

11. Lei, L., et al., *Preparation and properties of amino-functional reduced graphene oxide/waterborne polyurethane hybrid emulsions.* Progress in organic coatings, 2016. 97: p. 19-27.

12. Saha, V., et al. *Synthesis and characterization of reduced graphene oxide reinforced polymer matrix composite.* in *IOP Conference Series: Materials Science and Engineering.* 2018. IOP Publishing.

13. Randviir, E.P., D.A. Brownson, and C.E. Banks, *A decade of graphene research: production, applications and outlook.* Materials Today, 2014. 17(9): p. 426-432.

14. Tkachev, S., et al., *Reduced graphene oxide.* Inorganic Materials, 2012. 48(8): p. 796-802.

15. Pei, S. and H.-M. Cheng, *The reduction of graphene oxide.* Carbon, 2012. 50(9): p. 3210-3228.

16. Wang, X. and M. Song, *Toughening of polymers by graphene.* Nanomaterials and Energy, 2013. 2(5): p. 265-278.

17. Yu, J., et al., *Current trends and challenges in the synthesis and applications of chitosan-based nanocomposites for plants: A review.* Carbohydrate Polymers, 2021. 261: p. 117904.

18. Dhahri, A., et al., *Chitosan-dithiooxamide-grafted rGO sheets decorated with Au nanoparticles: Synthesis, characterization and properties.* European Polymer Journal, 2016. 78: p. 153-162.

19. Ahmed, E.H., et al., *Nanocomposites dendritic polyamidoamine-based chitosan hyperbranched polymer embedded in silica–phosphate for waveguide applications.* Polymer-Plastics Technology and Materials, 2021. 60(7): p. 744-755.

20. Al-Remawi, M., *Application of N-hexoyl chitosan derivatives with high degree of substitution in the preparation of super-disintegrating pharmaceutical matrices.* Journal of Drug Delivery Science and Technology, 2015. 29: p. 31-41.

21. Chen, J., et al., *An improved Hummers method for eco-friendly synthesis of graphene oxide.* Carbon, 2013. 64: p. 225-229.

22. Xu, C., R.-s. Yuan, and X. Wang, *Selective reduction of graphene oxide.* New Carbon Materials, 2014. 29(1): p. 61-66.

23. Hossain, M. and A. Iqbal, *Production and characterization of chitosan from shrimp waste.* Journal of the Bangladesh Agricultural University, 2014. 12(1): p. 153-160.

24. Chen, Q., et al., *Study on the biodegradability of a chitosan‑modified hyperbranched polymer for enhanced oil recovery.* Journal of Applied Polymer Science, 2022. 139(1): p. 51425.

25. Triana-Guzmán, V.L., et al., *New chitosan-imine derivatives: from green chemistry to removal of heavy metals from water.* Revista Facultad de Ingeniería Universidad de Antioquia, 2018(89): p. 34-43.

26. Chen, Q., et al., *Synthesis and solution properties of a novel hyperbranched polymer based on chitosan for enhanced oil recovery.* Polymers, 2020. 12(9): p. 2130.

27. Yang, K., et al., *Graphene oxide nanofiltration membranes containing silver nanoparticles: Tuning separation efficiency via nanoparticle size.* Nanomaterials, 2020. 10(3): p. 454.

28. Du, Y.-c., et al., *Preparation of graphene oxide/silica hybrid composite membranes and performance studies in water treatment.* Journal of Materials Science, 2020. 55(25): p. 11188-11202.

29. Hasan, A.M., M. Keshawy, and M.E.-S. Abdel-Raouf, *Atomic force microscopy investigation of smart superabsorbent*

hydrogels based on carboxymethyl guar gum: Surface topography and swelling properties. Materials Chemistry and Physics, 2022. 278: p. 125521.

30. Fang, S., et al., *Synthesis of chitosan derivative graft acrylic acid superabsorbent polymers and its application as water retaining agent.* International journal of biological macromolecules, 2018. 115: p. 754-761.

31. Thakur, S. and N. Karak, *Multi-stimuli responsive smart elastomeric hyperbranched polyurethane/reduced graphene oxide nanocomposites.* Journal of Materials Chemistry A, 2014. 2(36): p. 14867-14875.

32. Ogawa, K., K. Oka, and T. Yui, *X-ray study of chitosan-transition metal complexes.* Chemistry of materials, 1993. 5(5): p. 726-728.

33. Liu, C., et al., *Hyperbranched polytriazine grafted reduced graphene oxide and its application.* Journal of Polymer Science Part A: Polymer Chemistry, 2015. 53(18): p. 2132-2140.

34. Chen, Y., et al., *Synthesis and characterization of a novel superabsorbent polymer of N, O-carboxymethyl chitosan graft copolymerized with vinyl monomers.* Carbohydrate Polymers, 2009. 75(2): p. 287-292.

35. Ge, H. and S. Wang, *Thermal preparation of chitosan–acrylic acid superabsorbent: Optimization, characteristic and water absorbency.* Carbohydrate polymers, 2014. 113: p. 296-303.